

Cortical Neurons form a Functional Neuronal Network in a 3D Printed Reinforced Matrix

Dieter Janzen, Ezgi Bakirci, Annalena Wieland, Corinna Martin, Paul D. Dalton, and Carmen Villmann*


Impairments in neuronal circuits underly multiple neurodevelopmental and neurodegenerative disorders. 3D cell culture models enhance the complexity of *in vitro* systems and provide a microenvironment closer to the native situation than with 2D cultures. Such novel model systems will allow the assessment of neuronal network formation and their dysfunction under disease conditions. Here, mouse cortical neurons are cultured from embryonic day E17 within in a fiber-reinforced matrix. A soft Matrigel with a shear modulus of 31 ± 5.6 Pa is reinforced with scaffolds created by melt electrowriting, improving its mechanical properties and facilitating the handling. Cortical neurons display enhanced cell viability and the neuronal network maturation in 3D, estimated by staining of dendrites and synapses over 21 days *in vitro*, is faster in 3D compared to 2D cultures. Using functional readouts with electrophysiological recordings, different firing patterns of action potentials are observed, which are absent in the presence of the sodium channel blocker, tetrodotoxin. Voltage-gated sodium currents display a current–voltage relationship with a maximum peak current at -25 mV. With its high customizability in terms of scaffold reinforcement and soft matrix formulation, this approach represents a new tool to study neuronal networks in 3D under normal and, potentially, disease conditions.

3D *in vitro* cell culture models are becoming more and more important as they attempt to recreate the *in vivo* microenvironment of cells. The field of neuroscience is no exception with

D. Janzen, Dr. C. Martin, Prof. C. Villmann
Institute for Clinical Neurobiology
University Hospital Würzburg
Versbacherstr. 5, Würzburg 97078, Germany
E-mail: Villmann_C@ukw.de

E. Bakirci, Prof. P. D. Dalton
Department of Functional Materials in Medicine and Dentistry
and Bavarian Polymer Institute
University Hospital Würzburg
Pleicherwall 2, Würzburg 97070, Germany

A. Wieland
Department of Obstetrics and Gynecology
University Hospital Erlangen
Laboratory for Molecular Medicine
FAU Erlangen-Nürnberg
Universitätsstrasse, 21–23, Erlangen 91054, Germany

 The ORCID identification number(s) for the author(s) of this article can be found under <https://doi.org/10.1002/adhm.201901630>.

© 2020 The Authors. Published by WILEY-VCH Verlag GmbH & Co. KGaA, Weinheim. This is an open access article under the terms of the Creative Commons Attribution-NonCommercial License, which permits use, distribution and reproduction in any medium, provided the original work is properly cited and is not used for commercial purposes.

DOI: 10.1002/adhm.201901630

the third dimension especially important for neuronal outgrowth and thus dendritic arborization. Such 3D neuronal cultures have been described in various hydrogels/matrices and scaffolds.^[1] Some common matrices are agarose,^[2] alginate,^[3,4] collagen,^[5,6] and Matrigel^[7] while peptides derived from extracellular matrix (ECM) proteins such as laminin (RGD, YIGSR, IKVAV) are often used to influence cell behavior.^[8] Alongside variables like growth factors and ECM proteins, matrix stiffness is an important factor when trying to create an *in vitro* 3D neuronal model that is intended to mimic the *in vivo* situation.^[9] Brain tissue is extremely soft, with reported elastic moduli ranging from 30–500 Pa, depending on brain region and developmental stage.^[10] Stiffness gradients are detected by neurons and used as guidance cues, affecting growth direction and neurite length.^[3,11] Mimicking soft brain tissue requires equally soft matrices,

which are difficult to handle and easily destroyed, for example, when performing immunocytochemical staining. One solution to this problem is the fiber-reinforcement of soft matrices.

Melt electrowriting (MEW) is a relatively new additive manufacturing technology^[12] and can fabricate highly porous (>90 vol%) reinforcing frames.^[13] Such MEW-reinforced cell-containing matrices have been used in strong and tough biomaterials for cartilage^[13] and vascular applications.^[14] The placement of the fibers, and whether they are linear or sinusoidal can significantly influence the mechanics and porosity of the hydrogel composite.^[15] Mechanical properties and biological response to the scaffolds could therefore be adjusted with the internal architecture and hybrid scaffold design.^[12,14] Additionally, MEW uses no toxic solvents and scaffolds can be used almost immediately within the biological framework.

Previously, we described how poly(ϵ -caprolactone) (PCL) scaffolds made via MEW could be used for reinforcement of Matrigel.^[16] Using this technique, we created a 3D model that allowed 3D electrophysiology of a transfected fibroblast cell line.^[16] This study expands on this, to incorporate and perform 3D electrophysiology of neurons. Techniques were developed to prevent blockage of the patch pipette by the Matrigel, and to direct it toward a neuron to take recordings. Reinforcing PCL MEW frames with ten layers and a hatch spacing of 200 μ m were fabricated and used as 9 mm discs that fit into 24-well

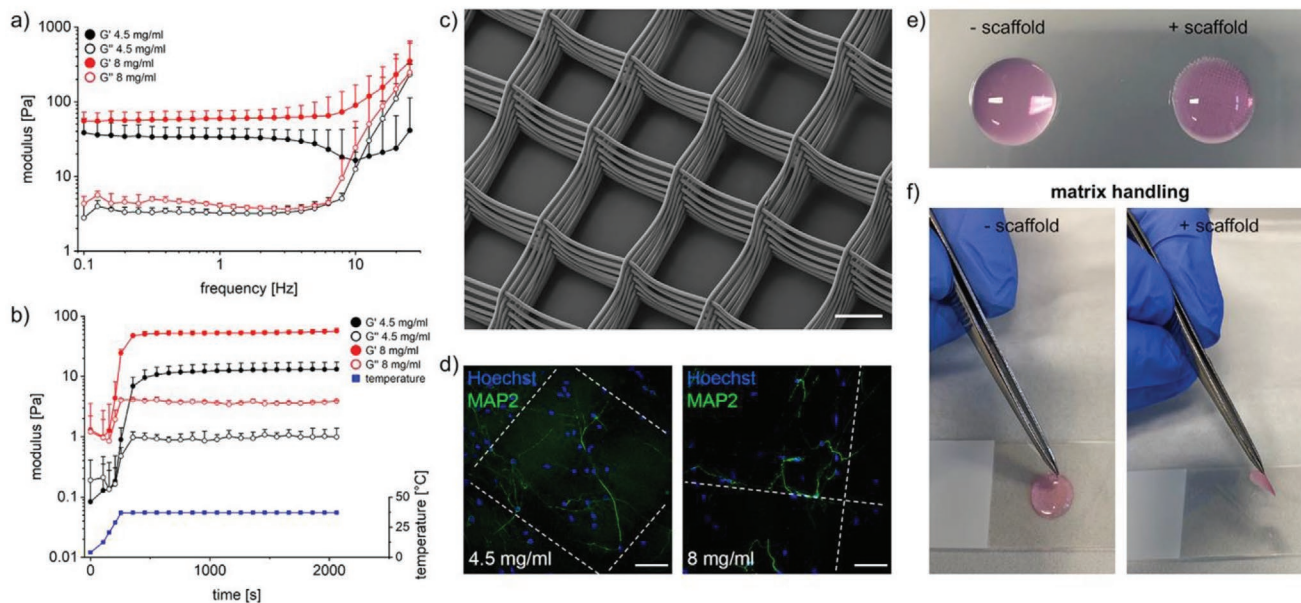


Figure 1. Rheological characterization of Matrigel at different concentrations. a) Frequency sweep and b) time sweep data comparing rheological storage (G') and loss moduli (G'') of 4.5 and 8 mg mL⁻¹ Matrigel. Error bars indicate standard deviation ($n = 3$ independent experiments). Lower graph exhibits the temperature plot (blue curve). c) Scanning electron microscopy image of MEW-scaffold with a hatch spacing of 200 μm , diameter of scaffolds is 9 mm. d) Cortical neurons at DIV7 using 4.5 and 8 mg mL⁻¹ Matrigel-scaffold composites ($n = 3$). Neurons were stained for MAP2 (green) and the nucleus (Hoechst, blue). White dotted lines indicate MEW fibers. Scale bar = 50 μm . e) Drop-like hydrogel (Matrigel 4.5 mg mL⁻¹) without (left) and with (right) scaffold. f) Handling properties of soft Matrigel without (left) and with (right) MEW scaffold. Note, the matrix without scaffold cannot be lifted with forceps. Presence of scaffold allows easy transfer with forceps.

plates. Since PCL is a slowly degrading polymer (2–3 years),^[17] it can be considered stable for the periods used in this study.

Rheological measurements of Matrigel with concentrations of 4.5 and 8 mg mL⁻¹ were performed without the MEW scaffold. Using an amplitude sweep at 1 Hz, the linear viscoelastic region of Matrigel was identified up to 1% strain (data not shown), therefore a lower strain of 0.1% was used to ensure deformation remains within the linear region. A frequency sweep of 0.1–30 Hz confirms crosslinking of Matrigel at both concentrations (Figure 1a). Values obtained from amplitude and frequency sweep were used for a time sweep to get a gelation profile of Matrigel at concentrations of 4.5 and 8 mg mL⁻¹ (Figure 1b, blue line). The final storage modulus of Matrigel was 31 ± 5.6 Pa for 4.5 mg mL⁻¹ and 66 ± 4.4 Pa for 8 mg mL⁻¹ concentrations, shown in Figure 1b with corresponding temperature profile used for gelation.

To exhibit neuronal network formation, mouse cortical neurons taken from embryonic stage E17 were seeded into MEW (Figure 1c) reinforced Matrigel of both concentrations (Figure 1d). The presence of MEW had no obvious impact on dendrite extend, orientation, and neuronal network formation within 21 days in vitro (DIV) of growth in 4.5 mg mL⁻¹ compared to 8 mg mL⁻¹ of Matrigel. Since embryonic neurons come from a rather soft environment, the following experiments were performed at the lower Matrigel concentration of 4.5 mg mL⁻¹. The presence of MEW, however enabled handling and easy transfer of the formed neuronal network in reinforced Matrigel for various experimental purposes (Figure 1e,f and Video S1, Supporting Information).

The cell viability of cortical neurons in reinforced Matrigel was measured at DIV1, 7, 14, and 21, Figure 2a). Viability was

high in 3D at DIV1 ($85 \pm 7\%$) and DIV7 ($83 \pm 6\%$) and significantly decreased after 2 (DIV14, $65 \pm 7\%$) and 3 (DIV21, $54 \pm 8\%$) weeks in culture (Figure 2b). Living cells also reduce over time in 2D neuronal cultures,^[18,19] however the number in 2D culture was already lower after 1 week (DIV7, $50 \pm 8\%$) than in 3D cultures after 3 weeks (Figure 2b). Immunocytochemical staining of cortical neurons was performed to visualize neuronal network formation in MEW scaffold reinforced Matrigel (Figure 2c). The dendritic marker MAP2 as well as the synaptic marker synaptophysin^[20] were used to specifically concentrate on synapse formation as an estimate of neuronal maturation. At DIV1, MAP2 and synaptophysin signals were limited to a few cells and located close to nuclei, as neurite formation was just beginning (Figure 2c,d). A widespread neuronal network with strong MAP2 and synaptophysin signal has been formed by DIV7 with further increased network density at DIV14 and DIV21. The 3D reconstruction of neurons within the fiber-reinforced matrix revealed a close proximity of both markers (Figure 2d and Video S2, Supporting Information). The quantification of the synaptophysin signal as an estimate for the number of synapses formed demonstrated a larger increase of synapse formation within the first 7 days in 3D compared to 2D cultures (3D: synaptophysin density/100 μm dendrite 15 ± 10 , $n = 26$; 2D 7.5 ± 7.5 , $n = 17$; Figure 2e). Furthermore, dendrites grew longer within the first week in 3D cultures compared to 2D cultures (3D: 86 ± 40 μm , $n = 39$); 2D: 56 ± 25 μm , $n = 25$, Figure 2f). Our results indicate that cortical neurons start to form a structural network after only DIV7 in 3D cultures.

To investigate the maturation level of the 3D neural network, calcium imaging was performed (Figure 3a and Video S3,

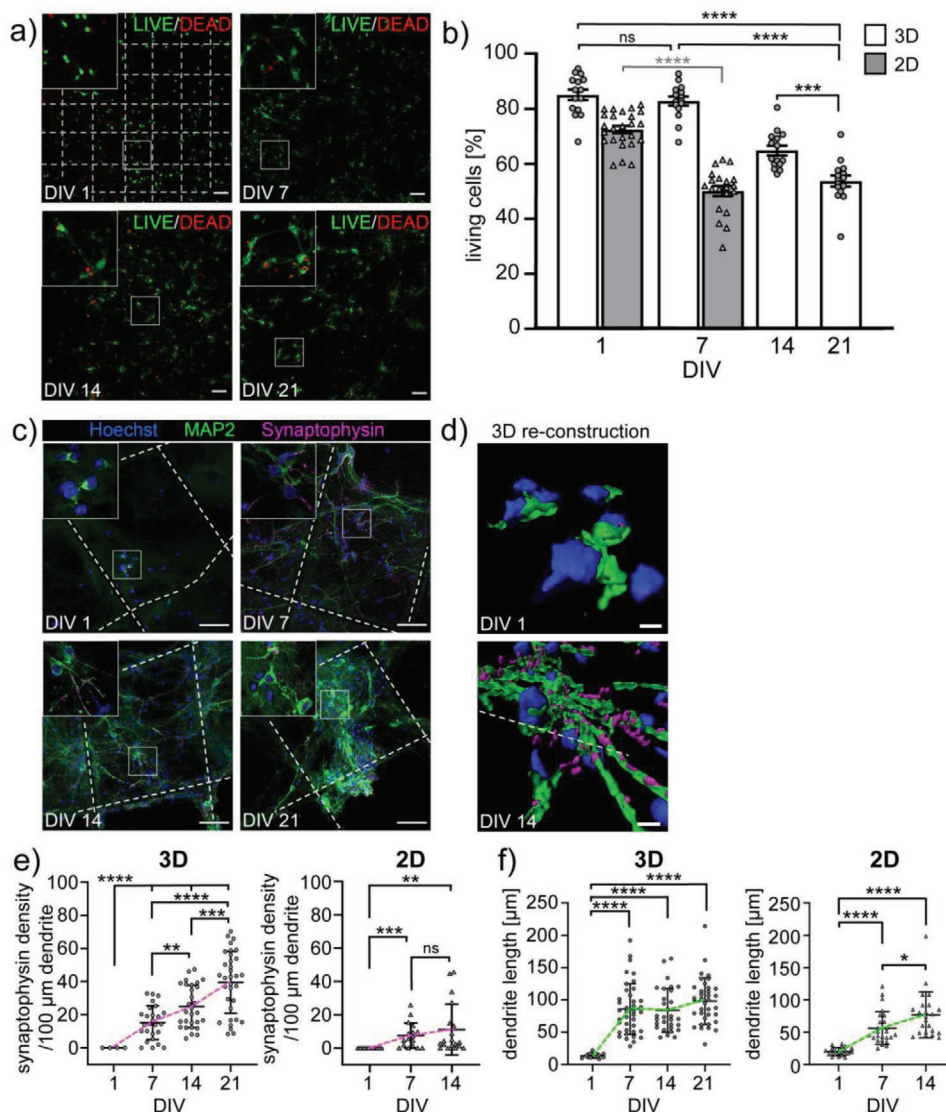


Figure 2. Cortical neurons commence network formation around DIV7 in 3D cultures. a) Cell viability assay of cortical neurons in 3D after DIV1, 7, 14, 21. Live cells are shown green; dead cells, red. Scale bar = 100 μm ; three independent experiments were performed $n = 3$. b) Cell viability was quantified by cell counting in five images per experiment. Living cells: white bars 3D, gray bars 2D. Note, the cell viability at DIV7 in 2D is lower compared to 3D cultures after 3 weeks in culture. Black asterisks refer to 3D viability, gray asterisks to 2D living cells, $***p < 0.001$, $****p < 0.0001$. c) Immunocytochemical staining of 3D cortical neurons in 4.5 mg mL^{-1} Matrigel-scaffold composites (MAP2, green; synaptophysin, magenta; nuclei (Hoechst), blue). White dotted lines indicate MEW fibers. Insets show a single $1 \mu\text{m}$ slice of the highlighted areas (white box). Scale bar = $50 \mu\text{m}$. d) 3D reconstruction of magnified areas from DIV1 and 14 seen in (c). e) Quantification of synaptophysin as a synaptic marker in 3D (circles) and 2D (triangles) cultures, pink dotted lines connect mean values, $n = 3$. f) Comparison of neurite length in 3D (circles) and 2D (triangles) cultures, green dotted lines connect mean values, $n = 3$. Values of significance in (e) and (f) $**p < 0.01$, $***p < 0.001$, $****p < 0.0001$, ns = non significant, error bars indicate standard deviation.

Supporting Information). Between DIV13–16 in 2D neuronal cultures, neuronal networks show synchronized network activity.^[21,22] At DIV14, spontaneous action potential firing was primarily observed which could be blocked by application of the sodium channel blocker TTX (Figure 3b). Hence, we used the time window between DIV14–18 to perform electrophysiological measurements from cortical neurons in 3D using the whole-cell configuration either in current or voltage-clamp mode.^[23] Neuronal cultures in scaffold reinforced Matrigel were transferred to a recording chamber and fixed with an O-ring.^[6] We used MEW fibers with a frame size of $200 \mu\text{m}$ which

displayed enough space for the recording pipette mounted in a 45° angle to reach cortical neurons not only at the top but also in deeper layers of the reinforced matrix.^[16] Positive pressure was applied to the patch pipette to prevent clogging with matrix while approaching a cell (Figure 3c). Occasionally, pressure was increased even further in short bursts to clear the cell of matrix (Video S4, Supporting Information). The rapid transmission of electrical signals and their conversion into chemical signals depends on the action of voltage-gated sodium channels (VGSCs). Voltage-gated sodium currents were recorded using 10 mV steps from -80 mV to $+40 \text{ mV}$ ($n = 6$, Figure 3d). The

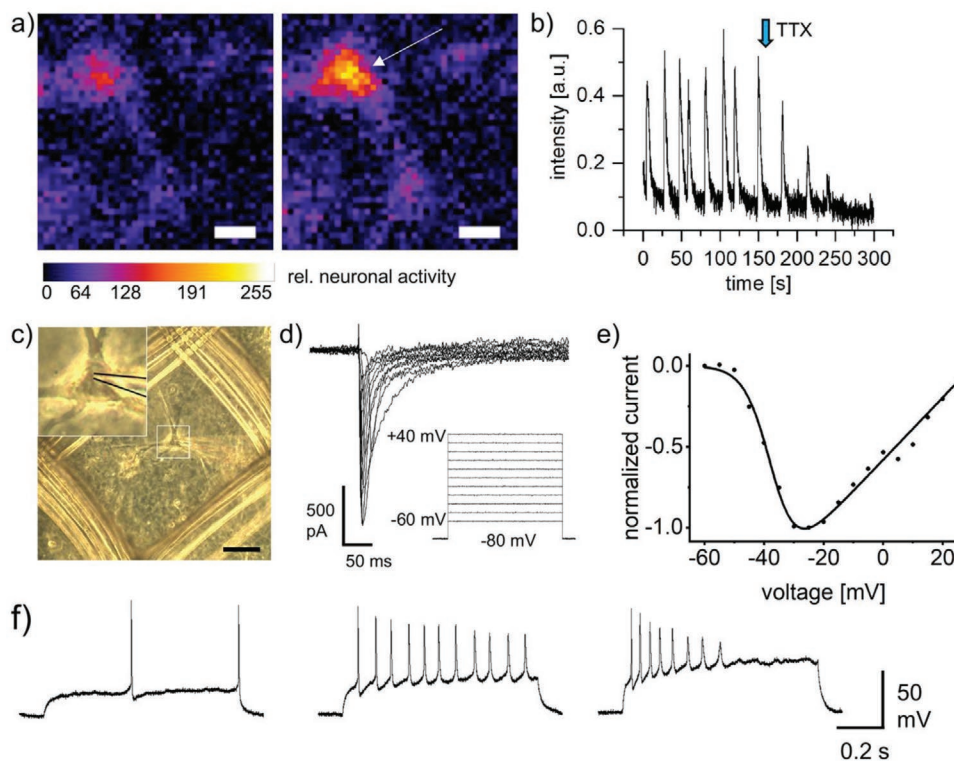


Figure 3. Cortical neurons grown in scaffold reinforced Matrigel exhibit neuronal network activity. a) Calcium imaging of cortical neurons in reinforced matrix at DIV14. Same cell without (left) and with (right) neuronal activity. Relative neuronal activity is shown by color code from dark blue (no activity) to yellow (high activity). White bar refers to 10 μm . b) Spontaneous action potential firing of cortical neurons in reinforced Matrigel over a time course of 300 s. Application of the sodium channel blocker tetrodotoxin (TTX) to block neuronal activity is marked by blue arrow. c) Cortical neuron in MEW scaffold reinforced Matrigel. Inset shows magnification with the patch pipette (traced in black) approaching the cell. Scale bar = 50 μm . d) Representative traces of voltage-gated sodium channel recordings at voltages from -80 to $+40$ mV, $n = 6$. e) Typical current–voltage relationship of voltage-gated sodium channels with the largest amplitude at -25 mV. f) Current clamp recordings of action potentials from DIV18 cortical neurons. An increasing current was injected for 800 ms in 10 pA steps. Depolarization above threshold evokes single APs (top). Strong depolarization results in repetitive firing (middle) and eventually a complete blockage (bottom).

current–voltage relationship showed maximum sodium currents at -25 mV (Figure 3e).^[24]

After achieving the whole-cell configuration, action potentials were recorded in current clamp mode by injection of 10 pA current steps starting at a membrane potential of -80 mV. Current injection to a near-threshold potential evoked single action potentials (Figure 3f, left trace). Further current injection resulted in repetitive firing and eventually, blockage of action potentials (Figure 3f, middle and right trace). Similar firing patterns have been reported before for cortical pyramidal neurons.^[25]

Action potential firing argues for functional neuronal network formation.^[19,22,26] To exhibit functional neuronal networks with synchronized activity, the initial cell density during seeding is important.^[27] While we have tested densities of 5400–16200 cells mm^{-3} , the optimal cell density was estimated to 10 800 cells mm^{-3} .

Previously, we described a transfected cell line embedded in MEW scaffold reinforced Matrigel and electrophysiological recordings of a transfected ligand-gated ion channel.^[16] Here, we successfully used this 3D cell culture approach to study primary cortical neurons, demonstrating that this model achieves the state of a mature functional neuronal network after 2 weeks

in culture with better cell survival, faster dendrite growth and synapse formation within the first week in culture compared to 2D cultures. This model could be further improved by replacing Matrigel with matrices specifically tailored for the desired cell type. Full control over mechanical support and matrix formulation will allow creation of an optimal environment for studying growth and electrophysiological properties of cells of the central nervous system. The MEW scaffolds used here provide mechanical support for weak matrices comparable to the native embryonic brain environment and allow sufficient handling to study neuronal cell types under healthy and, potentially, disease conditions.

Experimental Section

MEW Process: A custom-built MEW printer^[28] was used to fabricate scaffolds as previously described.^[16] Briefly, MEW was performed using medical-grade PCL (PURASORB PC 12, Lot#1712002224, 05/2018; Corbion Inc, Amsterdam, Netherlands) at 21 ± 2 °C and a humidity of $35 \pm 10\%$. The following parameters were used: heating to 80 °C; 3 bar of air pressure; 25G nozzle; 6 kV voltage applied across a 4 mm collector distance. A 48×96 mm rectangular mesh with ten layers and 200 μm fiber spacing was direct-written and cut to 9 mm disks with an infrared laser.

Mechanical Behavior: Rheological characterization of Matrigel was performed using a Physica MCR 301 rheometer (Anton Paar, Graz, Austria) with a parallel plate configuration (25 mm diameter, 0.5 mm gap size). Matrigel samples (500 μL ; 4.5 or 8 mg mL^{-1}) were loaded onto the lower plate at 4 $^{\circ}\text{C}$.^[16] The amplitude sweep was performed between 0.01% and 100% strain at 1 Hz. According to amplitude sweep results, linear viscoelastic regions were defined, and the frequency sweep was performed between 1 and 30 Hz at 0.1% strain. Samples were exposed to 1 Hz frequency and 0.1% strain to understand time and temperature dependent behavior during heating from 4 to 37 $^{\circ}\text{C}$ at a rate of 10 $^{\circ}\text{C min}^{-1}$ and setting at 37 $^{\circ}\text{C}$ for 30 min. All experiments were performed in triplicates.

Isolation of Cortical Neurons: Primary cortical neuronal cultures were prepared at E17 from CD1 mouse embryos. Experiments were authorized by the local veterinary authority and Committee on the Ethics of Animal Experiments (Regierung von Unterfranken). Briefly, cortices were incubated with 0.5 mg mL^{-1} trypsin, 0.2 mg mL^{-1} EDTA, and 10 $\mu\text{g mL}^{-1}$ DNase I in PBS for 30 min at 37 $^{\circ}\text{C}$. Trypsinization was stopped by adding 10% fetal calf serum. Cells were dissociated by trituration and counted.

Scaffold Preparation, Cell Seeding, and Culture: MEW scaffolds in 24-well plates were washed once with 70% ethanol, three times with ddH₂O, and once with PBS. A cell suspension containing 200 000 cells and Matrigel (Corning, NY, USA) were mixed to a final volume of 180 μL and a protein concentration of 4.5 or 8 mg mL^{-1} and pipetted onto scaffolds. After 30 min of incubation at 37 $^{\circ}\text{C}$, 500 μL Neurobasal medium containing 2×10^{-3} M GlutaMAX and 2% (v/v) B27 supplement was added (Thermo Fisher Scientific, Waltham, MA, USA). For 2D cultures, 150 000 cells were seeded on poly-D-lysine coated glass cover slips. Cortical neurons were cultured in 2D and 3D under standard growth conditions at 37 $^{\circ}\text{C}$ and 5% CO₂. As neurons secrete growth factors by themselves into the cell culture medium and thus promote their growth, only 50% of fresh medium was added every week.^[29]

Cell Viability: The viability of cortical neurons was assessed 1, 7, 14, and 21 DIV after seeding. In brief, cells were incubated for 30 min at 21 $^{\circ}\text{C}$ for 30 min with 2×10^{-6} M Calcein-AM (green/living cells; Thermo Fisher Scientific, Waltham, MA, USA) and 2×10^{-6} M ethidium homodimer 1 (red/dead cells; Sigma-Aldrich, St. Louis, MO, USA) in PBS. Per time point, five images of at least three independent samples were used for determining the live/dead ratio. Cell viability numbers were acquired using the Spots model of Imaris 7.7.2 (Oxford Instruments, Abingdon, UK).

Immunocytochemical Staining: Cortical neurons were stained for microtubule-associated protein 2 (MAP2) and synaptophysin to assess network formation. All steps were performed at 21 $^{\circ}\text{C}$. Cells were fixed for 10 min with 2% formaldehyde, washed with PBS, and blocked/permeabilized for 3 min with 5% goat serum and 0.2% Triton X-100 in PBS. Cells were incubated with primary antibodies Anti-MAP2 and Anti-Synaptophysin for 1h (both 1:500; MAB3418, AB9272, Merck Millipore, Burlington, MA, USA). Following washing, cells were incubated for 45 min with secondary Alexa488-goat-anti-mouse and Cy3-goat-anti-rabbit antibodies (both 1:500; Dianova, Hamburg, Germany). Cells were mounted on glass slides with Hoechst 33342-containing ProLong Glass Antifade Mountant (Thermo Fisher Scientific, Waltham, MA, USA). Synaptophysin density was determined by tracing dendrites with the ImageJ plugin NeuronJ and subsequent counting of synaptophysin signal close to traced dendrites using SynapCountJ.^[30] Dendrite length was measured with the FilamentTracer of Imaris (Oxford Instruments, Abingdon, UK). Only the longest and fully traceable dendrites in each image were analyzed.

Confocal Microscopy and Image Acquisition: Cell viability and fluorescence images were acquired using an Olympus IX81 microscope equipped with a FV1000 confocal laser scanning system, a FVD10 SPD spectral detector, and diode lasers of 405, 495, 550, and 635 nm (Olympus, Tokyo, Japan). Olympus UPLSAPO 10 \times (air, numerical aperture 0.4) and UPLFLN 40 \times (oil, numerical aperture 1.3) objectives were used. Phase-contrast images were acquired using a Zeiss Axio Observer D1 microscope (Carl Zeiss AG, Oberkochen, Germany)

equipped with a Moticam 3+ (Motic Europe, Wetzlar, Germany). Images were processed with ImageJ/Fiji 1.52n using maximum intensity projection and display range adjustment.^[31] Imaris was used for 3D reconstruction (Oxford Instruments, Abingdon, UK).

Calcium Imaging: For cell calcium analysis, cortical neurons were labeled with the high affinity calcium indicator Oregon Green 488 BAPTA-1AM (Thermo Fischer Scientific, Waltham, MA, USA). 0.5 μL of a 5 mM stock solution in 20% Pluronic F-127 in DMSO was solved in 500 μL imaging solution for 30 min at 37 $^{\circ}\text{C}$ and 5% CO₂. The imaging solution consisted of (in $\times 10^{-3}$ M) 119 NaCl, 4.5 KCl, 1 MgCl₂, 2 CaCl₂, 1.2 NaH₂PO₄, 26 NaHCO₃, 10 glucose, 10 HEPES, pH7.4, adjusted with NaOH. Calcium imaging was performed under continuous perfusion with the imaging solution and TTX (550 nM) was applied using this perfusion system. Image series were captured at 10 Hz with a Rolera XR Mono fast 1394 CCD camera (Qimaging, Surrey, Canada) and StreamPix4 Software (Norpix, Montreal, Canada) under continuous illumination with a cooled epifluorescent light source for 470 nm (Visitron Systems, Puchheim, Germany) and analyzed by ImageJ.

Electrophysiology: The patch clamp technique was used to obtain whole-cell recordings of cortical neurons cultured in 3D for 14–21 days. Recording pipettes (2–3 M Ω) were pulled from thin-walled borosilicate capillaries (TW150F-4; World Precision Instruments, Sarasota, FL, USA) using a Sutter P97 horizontal puller (Sutter Instrument, Novato, CA, USA). Recordings were obtained with an EPC10 USB amplifier controlled by Patchmaster software (HEKA Elektronik, Lambrecht, Germany). Currents were low-pass filtered at 2.9 kHz and digitized at 20 kHz. For measurement of action potentials, the intracellular solution consisted of (in $\times 10^{-3}$ M) 130 KCl, 1 CaCl₂, 1 MgCl₂, 10 HEPES, 11 EGTA; pH 7.3, adjusted with KOH (294 ± 1.5 mOsm L⁻¹) and extracellular solution contained (in $\times 10^{-3}$ M): 140 NaCl, 1 CaCl₂, 1 MgCl₂, 10 HEPES; pH 7.3, adjusted with NaOH (305 ± 1.5 mOsm L⁻¹). A liquid junction potential of 5 mV was corrected, and cells were held at -70 mV. For measuring voltage-gated sodium channels, the intracellular solution contained (in $\times 10^{-3}$ M) 120 CsF, 5 NaCl, 1 CaCl₂, 1 MgCl₂, 10 HEPES, 11 EGTA, 2 Mg-ATP, 5 TEA-Cl; pH 7.3, adjusted with CsOH (303 ± 1.5 mOsm L⁻¹) and the extracellular solution consisted of (in $\times 10^{-3}$ M): 140 NaCl, 1 CaCl₂, 1 MgCl₂, 10 HEPES, 0.5 CdCl₂; pH 7.3, adjusted with NaOH (310 ± 1.5 mOsm L⁻¹). A liquid junction potential of 9 mV was corrected, and cells were held at -80 mV. R_s was compensated 80% to minimize voltage errors. The P/5 protocol was used to subtract leak currents and voltage.

Statistical Analysis: GraphPad Prism 8.3.0 (Graphpad Software, San Diego, CA, USA) was used to calculate mean values, standard deviation (SD), standard error of the mean, and values for statistical significance. Statistical significance was estimated using an unpaired *t* test with Welch's correction with **p* < 0.05, ***p* < 0.01, ****p* < 0.001, *****p* < 0.0001.

Supporting Information

Supporting Information is available from the Wiley Online Library or from the author.

Acknowledgements

This work was funded by the Deutsche Forschungsgemeinschaft (DFG, German Research Foundation)—Project number 326998133—TRR 225 (subproject B01). The technical assistance of Mr. Andrei Hrynevich is greatly appreciated.

Conflict of Interest

The authors declare no conflict of interest.

Keywords

3D electrophysiology, 3D neuronal networks, cortical neurons, melt electrowriting

Received: November 15, 2019

Revised: February 17, 2020

Published online: March 17, 2020

- [1] a) K. Chwalek, M. D. Tang-Schomer, F. G. Omenetto, D. L. Kaplan, *Nat. Protoc.* **2015**, *10*, 1362; b) M. F. Daud, K. C. Pawar, F. Claeysens, A. J. Ryan, J. W. Haycock, *Biomaterials* **2012**, *33*, 5901; c) A. R. Murphy, J. M. Haynes, A. L. Laslett, N. R. Cameron, C. M. O'Brien, *Acta Biomater.* **2019**, *101*, 102; d) S. K. Seidlits, J. Liang, R. D. Bierman, A. Sohrabi, J. Karam, S. M. Holley, C. Cepeda, C. M. Walthers, *J. Biomed. Mater. Res., Part A* **2019**, *107*, 704.
- [2] a) A. P. Balgude, X. Yu, A. Szymanski, R. V. Bellamkonda, *Biomaterials* **2001**, *22*, 1077; b) R. Bellamkonda, J. P. Ranieri, N. Bouche, P. Aebischer, *J. Biomed. Mater. Res.* **1995**, *29*, 663.
- [3] G. Palazzolo, N. Broguiere, O. Cenciarelli, H. Dermutz, M. Zenobi-Wong, *Tissue Eng., Part A* **2015**, *21*, 2177.
- [4] J. P. Frampton, M. R. Hynd, M. L. Shuler, W. Shain, *Biomed. Mater.* **2011**, *6*, 015002.
- [5] N. Dubey, P. C. Letourneau, R. T. Tranquillo, *Exp. Neurol.* **1999**, *158*, 338.
- [6] T. Xu, P. Molnar, C. Gregory, M. Das, T. Boland, J. J. Hickman, *Biomaterials* **2009**, *30*, 4377.
- [7] J. Park, I. Wetzel, I. Marriott, D. Dreau, C. D'Avanzo, D. Y. Kim, R. E. Tanzi, H. Cho, *Nat. Neurosci.* **2018**, *21*, 941.
- [8] a) P. D. Dalton, J. Mey, *Front. Biosci.* **2009**, *14*, 769; b) J. C. Schense, J. Bloch, P. Aebischer, J. A. Hubbell, *Nat. Biotechnol.* **2000**, *18*, 415; c) J. C. Schense, J. A. Hubbell, *J. Biol. Chem.* **2000**, *275*, 6813.
- [9] a) E. H. Barriga, K. Franze, G. Charras, R. Mayor, *Nature* **2018**, *554*, 523; b) E. Moeendarbary, I. P. Weber, G. K. Sheridan, D. E. Koser, S. Soleman, B. Haenzi, E. J. Bradbury, J. Fawcett, K. Franze, *Nat. Commun.* **2017**, *8*, 14787.
- [10] a) A. F. Christ, K. Franze, H. Gautier, P. Moshayedi, J. Fawcett, R. J. Franklin, R. T. Karadottir, J. Guck, *J. Biomech.* **2010**, *43*, 2986; b) M. Iwashita, N. Kataoka, K. Toida, Y. Kosodo, *Development* **2014**, *141*, 3793.
- [11] D. E. Koser, A. J. Thompson, S. K. Foster, A. Dwivedy, E. K. Pillai, G. K. Sheridan, H. Svoboda, M. Viana, L. D. Costa, J. Guck, C. E. Holt, K. Franze, *Nat. Neurosci.* **2016**, *19*, 1592.
- [12] T. M. Robinson, D. W. Huttmacher, P. D. Dalton, *Adv. Funct. Mater.* **2019**, *29*, 1904664.
- [13] J. Visser, F. P. Melchels, J. E. Jeon, E. M. van Bussel, L. S. Kimpton, H. M. Byrne, W. J. Dhert, P. D. Dalton, D. W. Huttmacher, J. Malda, *Nat. Commun.* **2015**, *6*, 6933.
- [14] N. T. Saïdy, F. Wolf, O. Bas, H. Keijndener, D. W. Huttmacher, P. Mela, E. M. De-Juan-Pardo, *Small* **2019**, *15*, 1900873.
- [15] O. Bas, D. D'Angella, J. G. Baldwin, N. J. Castro, F. M. Wunner, N. T. Saïdy, S. Kollmannsberger, A. Reali, E. Rank, E. M. De-Juan-Pardo, D. W. Huttmacher, *ACS Appl. Mater. Interfaces* **2017**, *9*, 29430.
- [16] N. Schaefer, D. Janzen, E. Bakirci, A. Hrynevich, P. D. Dalton, C. Villmann, *Adv. Healthcare Mater.* **2019**, *8*, 1801226.
- [17] M. Bartnikowski, T. R. Dargaville, S. Ivanovski, D. W. Huttmacher, *Prog. Polym. Sci.* **2019**, *96*, 1.
- [18] T. Voigt, H. Baier, A. Dolabela de Lima, *Eur. J. Neurosci.* **1997**, *9*, 990.
- [19] T. Opitz, A. D. De Lima, T. Voigt, *J. Neurophysiol.* **2002**, *88*, 2196.
- [20] G. Kierstein, K. Obst, P. Wahle, *Dev. Brain Res.* **1996**, *92*, 39.
- [21] a) T. A. Basarsky, V. Parpura, P. G. Haydon, *J. Neurosci.* **1994**, *14*, 6402; b) R. Blum, C. Heinrich, R. Sanchez, A. Lepier, E. D. Gundelfinger, B. Berninger, M. Gotz, *Cereb. Cortex* **2011**, *21*, 413; c) T. L. Fletcher, P. De Camilli, G. Banker, *J. Neurosci.* **1994**, *14*, 6695.
- [22] T. Voigt, T. Opitz, A. D. de Lima, *J. Neurosci.* **2005**, *25*, 4605.
- [23] M. Lindau, E. Neher, *Pflügers Arch.* **1988**, *411*, 137.
- [24] a) L. S. Milescu, B. P. Bean, J. C. Smith, *J. Neurosci.* **2010**, *30*, 7740; b) T. R. Cummins, F. Aglieco, M. Renganathan, R. I. Herzog, S. D. Dib-Hajj, S. G. Waxman, *J. Neurosci.* **2001**, *21*, 5952.
- [25] O. P. Hamill, J. R. Huguenard, D. A. Prince, *Cereb. Cortex* **1991**, *1*, 48.
- [26] D. Lam, H. A. Enright, J. Cadena, S. K. G. Peters, A. P. Sales, J. J. Osburn, D. A. Soscia, K. S. Kulp, E. K. Wheeler, N. O. Fischer, *Sci. Rep.* **2019**, *9*, 4159.
- [27] a) M. Chiappalone, M. Bove, A. Vato, M. Tedesco, S. Martinoia, *Brain Res.* **2006**, *1093*, 41; b) R. Madhavan, Z. C. Chao, S. M. Potter, *Phys. Biol.* **2007**, *4*, 181.
- [28] T. D. Brown, P. D. Dalton, D. W. Huttmacher, *Adv. Mater.* **2011**, *23*, 5651.
- [29] S. Majd, A. Zarifkar, K. Rastegar, M. A. Takhshid, *Iran. Biomed. J.* **2008**, *12*, 101.
- [30] E. Meijering, M. Jacob, J. C. Sarria, P. Steiner, H. Hirling, M. Unser, *Cytometry* **2004**, *58A*, 167.
- [31] J. Schindelin, I. Arganda-Carreras, E. Frise, V. Kaynig, M. Longair, T. Pietzsch, S. Preibisch, C. Rueden, S. Saalfeld, B. Schmid, J. Y. Tinevez, D. J. White, V. Hartenstein, K. Eliceiri, P. Tomancak, A. Cardona, *Nat. Methods* **2012**, *9*, 676.